

Silicon-Based Monolithic 4×4 Wavelength-Selective Cross Connect with On-Chip Micromirrors

Chao-Hsi Chi^{1,2}, Jui-Che Tsai³, Dooyoung Hah⁴, Sagi Mathai¹, Ming-Chang M. Lee⁵, and Ming C. Wu¹

¹ Berkeley Sensors & Actuators Center (BSAC) and Department of Electrical Engineering and Computer Sciences
University of California, Berkeley, California 94720, USA
E-mail: chaohsi@ucla.edu

² Department of Electrical Engineering, University of California, Los Angeles, California 90095, USA

³ Graduate Institute of Electro-Optical Engineering, National Taiwan University, Taiwan

⁴ Department of Electrical and Computer Engineering, Louisiana State University, Louisiana 70803, USA

⁵ Department of Electrical Engineering and Institute of Photonics Technologies, National Tsing Hua University, Taiwan

Abstract: A monolithic 4×4 wavelength-selective cross-connect (chip area = 3.2×4.6 cm²) is realized by integrating four 4×1 MEMS wavelength-selective switches and four 1×4 passive splitters, together with a 4×4 waveguide shuffle network on a silicon-on-insulator. Wavelength-selective routing has been successfully demonstrated.

©2006 Optical Society of America

OCIS codes: (060.1810) Couplers, switches, and multiplexers; (060.4510) Optical communications

1. Introduction

1×N wavelength-selective switch (WSS) and N×N wavelength-selective cross connect (WSXC) are key enabling elements for reconfigurable optical networks. Free-space MEMS (micro-electro-mechanical-systems) WSS [1-4] and WSXC [5] offer many advantages, including high port count, low insertion loss and crosstalk, optical transparency, and polarization insensitivity. However, their sizes are often limited by the bulk optical elements (such as lenses, gratings, etc.) and the long free-space propagation distances. Optical alignment and assembly are also cumbersome processes.

Compact switches can be realized by combining MEMS components and planar lightwave circuits (PLC) [6]. Hybrid WSS's have been demonstrated using arrayed waveguide grating (AWG) and external MEMS micromirrors [7,8]. However, those WSS's still require bulk lenses between the PLC and the micromirrors for collimation and focusing. Complicated optical alignment and mechanical assembly are also needed.

We have previously reported on a monolithic 1×4 MEMS WSS for coarse wavelength-division-multiplexing (CWDM) networks [9]. The MEMS micromirrors, diffraction gratings, and silicon PLC are monolithically fabricated on a silicon-on-insulator (SOI) substrate. The SOI platform is particularly attractive because they are compatible with Si PLC [10] as well as SOI-MEMS technologies. All optical paths are defined by photolithography and no optical alignment is necessary.

In this paper, we extend our previous work to a single-chip 4×4 WSXC fabricated on an SOI substrate. A 4×4 WSXC can be realized by cascading either four 1×4 and four 4×1 WSS's (Fig.1b) or four 1×4 splitters and four 4×1 WSS's (Fig. 1c). The latter has a fundamental splitting loss of 6 dB but it allows broadcast and multicast functions. It also has a smaller chip area (~ 60% of the 8-WSS approach), making it attractive for monolithic integration.

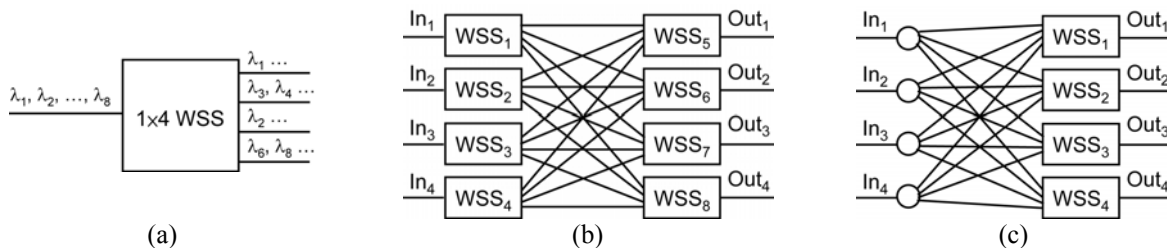


Fig. 1. Block diagrams of (a) 1×4 WSS with eight wavelength channels (b) 4×4 WSXC built with eight 1×4 WSS's (c) 4×4 WSXC built with four 1×4 passive splitters and four 4×1 WSS's.

2. Device Design and Simulation

The monolithic 1×4 WSS [9] is shown in Fig. 2a. The device consists of five 5μm-wide waveguides, each integrated with a collimating reflector and a micro-grating [11], a focusing reflector, and an 8-element micromirror array

OTuF1.pdf

matching to the CWDM (1470-1610nm) grids with 20-nm spacing. The MEMS mirror is actuated by a rotary comb-drive actuator. Total internal reflection (TIR) is used for the collimating and the focusing reflectors. All silicon-air interfaces are anti-reflection (AR)-coated by 180-nm-thick low-stress silicon nitride ($n = 2.15$). The micromirror is coated with aluminum to enhance its reflectivity.

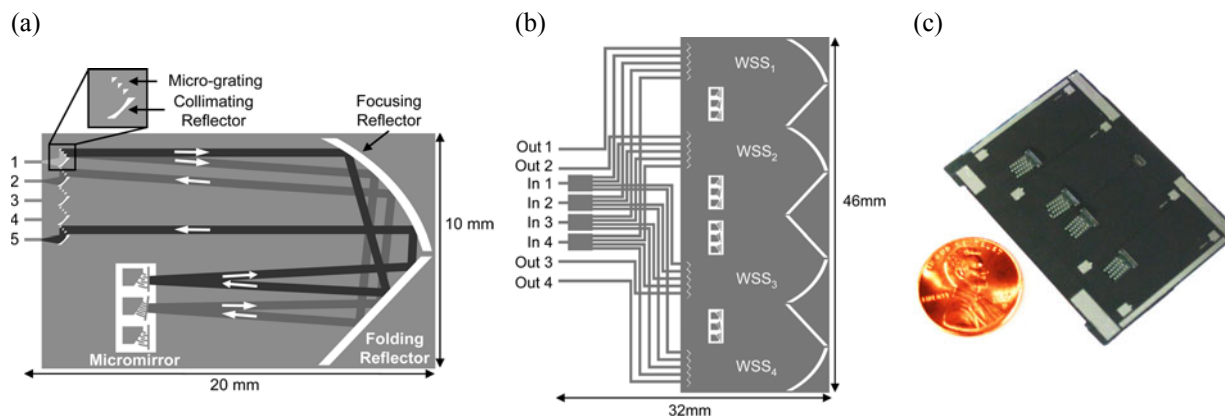


Fig. 2. (a) Schematic of the 1x4 MEMS WSS (b) Layout of the 4x4 WSXC (c) Fabricated 4x4 WSXC chip.

The 4x4 WSXC is realized by connecting four 4x1 WSS's and four 1x4 splitters with an integrated waveguide shuffle network (Fig. 2b). No fiber connections or external splitter are required. The 1x4 multimode interference (MMI) splitter is 890 μm long and 40 μm wide. The shuffle network employs 90° waveguide bend ($R = 100 \mu\text{m}$) and 90° waveguide crossing to minimize loss and crosstalk. The curved waveguide is offset laterally from the straight waveguide by 1 μm to optimize the mode-matching. The calculated optical loss is 0.02 dB/crossing and 1 dB/bend, respectively. The two lower WSS's are flipped vertically to reduce the number of waveguide crossings. There are no more than 10 crossing in any configuration.

3. Fabrication

The waveguides, parabolic mirrors, gratings, and on-chip MEMS micromirrors were patterned by optical lithography and then dry etched in an Applied Materials Precision 5000 etcher. The nitride was deposited by low-pressure chemical vapor deposition (LPCVD). Aluminum was deposited on the sidewall of MEMS micromirrors by e-beam evaporation with a 30° tilt angle. The backside of MEMS micromirror was etched by deep reactive ion etching (DRIE), followed by a dry release process, in which the buried oxide was removed by an Applied Materials Centura etcher. The chips were self-separated after dry release. No cleaving or dicing is needed. The fabricated 4x4 WSXC chip is shown in Fig. 2c. The fabricated chip size is 3.2x4.6 cm^2 .

4. Experimental Results

A lensed fiber array with 5 μm beam spot size was used to couple light to our 4x4 WSXC. An external cavity laser tunable from 1460nm to 1580nm was used as optical source. Figure 3a shows the optical insertion loss characterization by a static device with fixed mirror. Signals in In 1 was split and distributed to Port 2 of WSS₁ and WSS₂, and Port 5 of WSS₃ and WSS₄. At zero bias, the signals in WSS₃ and WSS₄ were reflected to Port 1, and then sent to Out 3 and Out 4. The fiber-to-fiber insertion loss was measured to be 24 dB, which includes the 6-dB splitting loss. The crosstalk is less than -25 dB.

Table 1 shows the breakdown of the insertion loss, which was measured on test structures fabricated on the same chip. The most critical parameter in fabrication is the verticality of the etched sidewalls. The measured 0.06 dB/TIR corresponds to a sidewall angle of 0.3°. The major discrepancy between theoretical and measured loss comes from the grating loss. Rounding and imperfect etching profile of the small triangular grating trench contributed to the extra losses. It could be improved by using reflective-type grating to reduce the loading effect.

Figure 3b shows the transfer curve (transmission-vs-voltage) of Out 4 with inputs from In 1, 2, 3, and 4, respectively. The maximum transmission occurs at 69V, 117V, 145V, 159V, respectively. The dependency of actuation voltage enables power equalization per port or per wavelength. Six micromirrors (mirror 3 to 8) have been tested with the available tuning wavelength range from 1460-1580nm. Fig. 3c shows the spectral response of switching from In 4 to Out 4 by scanning different micromirrors. The 3 dB passbands were identified as 1477-1482nm, 1488-1494nm, 1507-1517nm, 1527-1535nm, 1539-1553nm, and 1561-1573nm. An extra passband at <

OTuF1.pdf

1472nm was observed from adjacent grating order. We have also performed dynamic response of the MEMS switches. The temporal response time is on the order of ~ 0.5 msec.

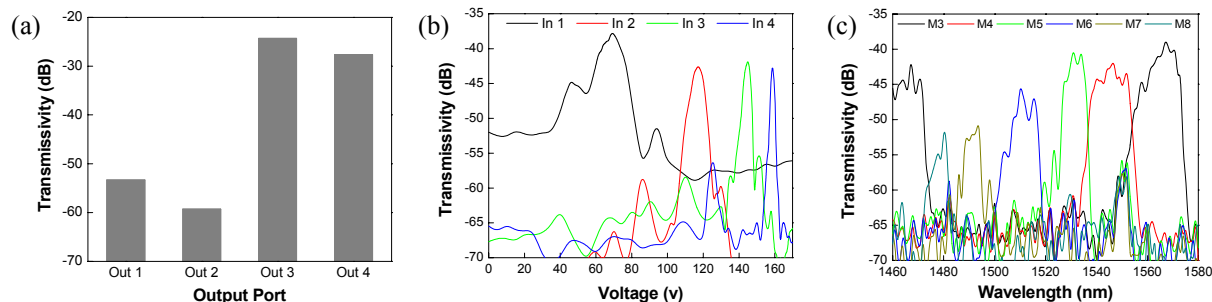


Fig. 3. (a) Measured insertion loss on a static 4x4 WSXC. (b) Transmissivity from the four input ports to Out 4 versus micromirror actuation voltage (c) Spectral response of In 4 to Out 4 by scanning mirror 3 (M3) to mirror 8 (M8).

Table 1. Estimation of insertion loss

Sources of Insertion Loss	Theoretical (Fundamental Limit)	Theoretical (Current Design)	Measured
Fiber Coupling $\times 2$	0.2	1.3	2.3
Sidewall Effect of TIR $\times 8$	0	0	0.5
Grating*	0	0	6
Diffraction (10 μm Air Gap)	2.3	2.3	2.8
Fresnel Loss (Imperfect AR Coating) $\times 4$	0	0.4	0.4
Total (1x4 WSS)	2.5	4.0	12
MMI	6	6	7.5 ~ 9
Bending $\times 4$	0	4	2
Crossing $\times 10$	0.2	0.2	0.5 ~ 1
Total (4x4 WSXC)	8.7	14.2	22 ~ 24

* Scalar behavior at central wavelength on the assumption of perfect blazing

5. Conclusion

We have reported on the design, fabrication, and experimental results of a single-chip 4x4 WSXC, realized by integrating four 1x4 splitters and four 4x1 WSS's. The Si planar lightwave circuits and the MEMS micromirrors are monolithically fabricated on a silicon-on-insulator (SOI) wafer. The resulting 4x4 WSXC has a chip area of 3.2×4.6 cm^2 . The breakdown of optical insertion loss is: 12 dB from the 1x4 WSS and 12 dB from the passive splitter and the waveguide shuffle network. Wavelength-selective routing has been demonstrated by scanning individual micromirrors. The power equalization per port or per wavelength can be realized by adjusting the actuation voltage. The monolithic WSXC can be scaled up to DWDM or with higher port counts.

This project is supported by DARPA CS-WDM program under MDA972-02-1-0020.

6. Reference

1. J. E. Ford, *et al.*, "Wavelength Add-Drop Switching Using Tilting Micromirrors," IEEE J. Light. Technol. **17**, 904-911 (1999)
2. Li Fan, *et al.*, "Digital MEMS switch for planar photonic crossconnects," Proc. of OFC 2002, TuO4
3. Sophia Huang, *et al.*, "Open-Loop Operation of MEMS WDM Routers with Analog Micromirror Array," Proc. of Optical MEMS 2002, ThD2
4. T. Ducellier, *et al.*, "The MWS 1x4: A High Performance Wavelength Switching Building Block," Proc. of ECOC 2002, 2.3.1
5. D. M. Marom, *et al.*, "64 Channel 4x4 Wavelength-Selective Cross-Connect for 40 Gb/s Channel Rates with 10 Tb/s Throughput Capacity," Proc. of ECOC 2003, We4.P.130
6. C. H. Chi, *et al.*, "Compact 1x8 MEMS optical switches using planar lightwave circuits," Proc. of OFC 2004, ThQ4
7. D. M. Marom, *et al.*, "Hybrid free-space and planar lightwave circuit wavelength-selective 1x3 switch with integrated drop-side demultiplexer," Proc. of ECOC 2005, Th3.6.4
8. T. Ducellier, *et al.*, "Novel High Performance Hybrid Waveguide-MEMS 1x9 Wavelength Selective Switch in a 32-Cascade Loop Experiment," Proc. of ECOC 2004, Th4.2.2
9. C. H. Chi, *et al.*, "Integrated 1x4 Wavelength-Selective Switch with On-Chip MEMS Micromirrors," Proc. of CLEO 2005, JThE58
10. B. Jalali, *et al.*, "Advances in Silicon-on-Insulator Optoelectronics," IEEE J. Sel. Top. Quantum Electron. **4**, 938-947 (1998)
11. C. N. Morgan, *et al.*, "Compact Integrated Silica Wavelength Filters," IEEE Photon. Technol. Lett. **14**, 1303-1305 (2002)